Chittaranjan Das[1]
G. A. Naganagowda[2]
Isabella L. Karle[3]
P. Balaram[1]

[1] *Molecular Biophysics Unit, Indian Institute of Science, Bangalore-560 012, India*

[2] *Sophisticated Instruments Facility, Indian Institute of Science, Bangalore-560 012, India*

[3] *Laboratory for the Structure of Matter, Naval Research Laboratory, Washington, DC 20375-5341, USA*

Designed β-Hairpin Peptides with Defined Tight Turn Stereochemistry

Abstract: *The conformational analysis of two synthetic octapeptides, Boc–Leu–Val–Val–D-Pro–L-Ala–Leu–Val–Val–OMe (**1**) and Boc–Leu–Val–Val–D-Pro–D-Ala–Leu–Val–Val–OMe (**2**) has been carried out in order to investigate the effect of β-turn stereochemistry on designed β-hairpin structures. Five hundred megahertz ^{1}H NMR studies establish that both peptides **1** and **2** adopt predominantly β-hairpin conformations in methanol solution. Specific nuclear Overhauser effects provide evidence for a type II′ β-turn conformation for the D-Pro–L-Ala segment in **1,** while the NMR data suggest that the type I′ D-Pro–D-Ala β-turn conformation predominates in peptide **2.** Evidence for a minor conformation in peptide **2,** in slow exchange on the NMR time scale, is also presented. Interstrand registry is demonstrated in both peptides **1** and **2.** The crystal structure of **1** reveals two independent molecules in the crystallographic asymmetric unit, both of which adopt β-hairpin conformations nucleated by D-Pro–L-Ala type II′ β-turns and are stabilized by three cross-strand hydrogen bonds. CD spectra for peptides **1** and **2** show marked differences, presumably as a consequence of the superposition of spectral bands arising from both β-turn and β-strand conformations.*

Keywords: *conformational analysis; synthetic octapeptides; stereochemistry; β-turn; β-strand; β-hairpin; crystal structure*

Correspondence to: Isabella L. Karle or P. Balaram

Sponsors: Department of Biotechnology, Government of India; National Institutes of Health (NIH) grant number: GM30902 and Office of Naval Research, USA.

INTRODUCTION

In an insightful analysis of β-hairpin structures in proteins, Sibanda and Thornton noted that polypeptide chain reversal was most often nucleated by tight turns of appropriate stereochemistry, which permitted correct registry of backbone hydrogen-bond donors and acceptors of adjacent antiparallel strands.[1] The preponderance of prime β-turns, type I′ and type II′, at the site of chain reversal has been confirmed in subsequent analyses with a larger data set of protein crystal structures.[2,3] The apparently stringent stereochemical requirements at the nucleating β-turn sites has been used to develop design strategies for constructing synthetic β-hairpin peptides. Both type I′ and II′ β-turns require positive values of the dihedral angle ϕ (N—C^{α}), $\sim +60°$ for the residue at the "$i + 1$" position of the turn; a condition that is met by using D-Pro at this position. In D-Pro, the constraints of pyrrolidine ring formation restricts ϕ to $\sim +60° \pm 20°$, facilitating both type I′ and II′ β-turn structures.[4] L-Asn, a residue with a high propensity to adopt positive ϕ values[5,6] has also been used in generating turn segments in synthetic β-hairpins.[7–9] The requirements at the "$i + 2$" position are more easily met, since in type II′ β-turns this residue must lie in the right-handed region of Ramachandran space, $\phi \sim -60° \pm 30°$, $\Psi \sim -30° \pm 30°$, a conformation that is readily accessible to all the protein amino acids. For the type I′ β-turn the "$i + 2$" residue must adopt a left-handed helical (α_L) conformation with, $\phi \sim +60° \pm 30°$, $\Psi \sim +30° \pm 30°$. Such a conformation requires that the "$i + 2$" position be occupied by an achiral residue, most often Gly, or a D-residue. Thus far, studies on synthetic β-hairpins focussed predominantly on D-Pro–Gly nucleating segments,[10–15] with a few examples of D-Pro–Xxx sequences[12,16–18] and Asn–Gly sequences.[7,9,19]

Recent studies have also focused on expanding on the number of atoms at the turn segments by incorporating β-amino acids[20,21] or higher omega amino acids.[22] In mimicking β-hairpins structures in proteins it would be desirable to establish design principles for generating hairpins nucleated with type I′ and II′ structures. In this report we compare the conformational properties of two acyclic octapeptides Boc–Leu–Val–Val–D-Pro–Xxx–Leu–Val–Val–OMe (Xxx = L-Ala **1,** Xxx = D-Ala **2;** Figure 1). The choice of sequences is dictated by previous studies that established a β-hairpin conformation in the solid state and in solution for the closely related octapeptide Boc–Leu–Val–Val–D-Pro–Gly–Leu–Val–Val–OMe (**3**).[13–15] In the D-Pro–Gly octapeptide a nucleating type II′ β-turn was observed under all conditions investigated. In peptides **1** and **2** the choice of L- and D-Ala at position 5 was dictated by the imperative to stabilize specific turn types. The results establish that peptide **1** adopts a β-hairpin conformation nucleated by a D-Pro–L-Ala type II′ β-turn, while peptide **2** (Xxx = D-Ala) shows a predominant population of β-hairpins, containing a type I′ D-Pro–D-Ala turn. NMR evidence suggests that in peptide **2** a minor population of hairpins nucleated by a type II′ β-turn also exists in solution. The crystal state conformation of peptide **1** confirms the β-hairpin structure.

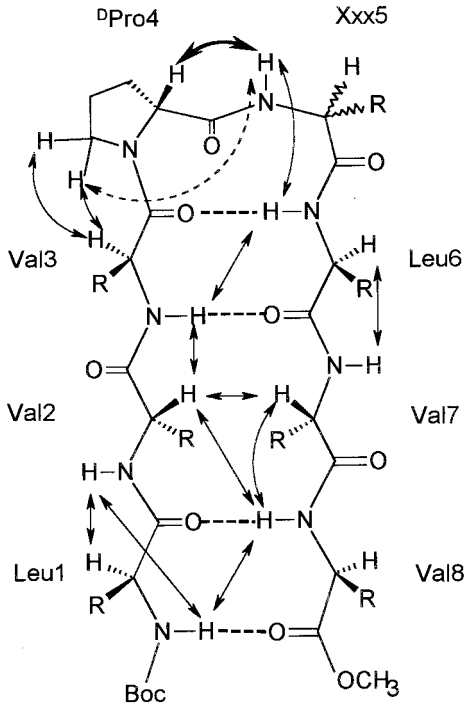

FIGURE 1 Schematic representation of the proposed β-hairpin structures of **1** (Xxx = L-Ala) and **2** (Xxx = D-Ala). The expected hydrogen bonds are shown by dashed lines. Observed NOEs are highlighted by double edged arrows. The dashed arrow indicates an observed NOE between $C^{\delta}H$ of D-Pro(4) and NH of D-Ala(5), which is diagnostic of a type I′ β-turn conformation in **2.** The thick arrow indicates the observed NOE between D-Pro(4) $C^{\alpha}H$ and L-Ala(5) NH characteristic of a type II′ β-turn conformation in **1.**

EXPERIMENTAL PROCEDURES

Peptide Synthesis

Peptides **1** and **2** were synthesized by conventional solution phase methods as described earlier[15] by using a fragment condensation strategy. The *t*-butyloxycarbonyl (Boc) group was used for N-terminal protection and the C-terminus was protected as a methyl ester. Deprotections were performed using 98% formic acid and saponification for N- and C-

terminus, respectively. Couplings were mediated by dicyclohexylcarbodiimide/1-hydroxybenzotriazole (DCC/HOBT). The final couplings of both the 8-residue peptides were achieved by the fragment condensation of Boc–Leu–Val–Val–OH and H–D-Pro–Xxx–Leu–Val–Val–OMe (Xxx = L-Ala/–D-Ala for peptide **1** and **2**), using DCC/HOBT as coupling agents. All the intermediates were characterized by ^{1}H NMR (80 MHz) and thin layer chromatography (TLC) on silica gel and used without further purification. The final peptides were purified by reverse phase, medium pressure liquid chromatography (C_{18}, 40–60 μ) and by high performance liquid chromatography (HPLC) on a reverse phase C_{18} column (5–10 μ, 7.8 × 250 mm) using methanol/water gradients. The purified peptides were analyzed by mass spectrometry on a Kratos PC-Kompact matrix-assisted laser desorption/ionization time of flight (MALDI-TOF) mass spectrometer: MNa^+_{obs} peptide **1,** 946.1 (M_{calc} 922.6); MNa^+_{obs} peptide **2,** 945.8 (M_{calc} 922.6). Both peptides were fully characterized by 500 MHz ^{1}H NMR.

NMR Spectroscopy

NMR studies were carried out on a Bruker DRX-500 spectrometer. All two-dimensional (2D) experiments were done in the phase-sensitive mode using time proportional phase incrementation. Double quantum filtered mass spectroscopy (DQF-COSY),[23] total COSY (TOCSY),[24] and rotating frame nuclear Overhauser effect spectroscopy (ROESY),[25,26] experiments were performed collecting 1 K data points in f2 and 512 data points in f1 using a spectral width of 5500 Hz. Solvent suppression was achieved using presaturation (using a 55 dB pulse in recycle delay of 1.5 s). Data were processed on a Silicon graphics Indy work station using Bruker XWIN NMR software. Typically, a sine squared window function, phase shifted by $\pi/2$ radians, was applied in both the dimensions. Data in f1 was zero filled to 1 K points. A spin–lock mixing time of 300 ms was used in ROESY experiments and a 70 ms mixing time was used for TOCSY experiments. The sample concentration was ~ 3 m*M* and the probe temperature was maintained at 300 K. Coupling constants were measured from resolution enhanced one dimensional spectra.

Structure Calculations

A total of 14 observed nuclear Overhauser effects (NOEs) for peptide **1,** and 16 NOEs for peptide **2** in methanol solution were used to derive upper limit distance restraints. NOEs were classified as strong (≤2.5 Å), medium (≤3.5 Å), and weak (≤4.5 Å), according to their intensities judged by visual inspection of contour levels. In addition to NOEs, 6 dihedral restraints from *J* values ($^3J_{C^\alpha H—NH}$ values ≥8.0 Hz used to restrain ϕ to −80° to −160°) were also used as inputs for structure calculations. A molecular dynamics calculation using the DISCOVER module available in INSIGHT II (Biosym, Inc.) was performed, with an extended starting conformation for 100,000 dynamic steps (100 ps). Structures at every 1000 steps were collected and used for further analysis. Ten out these structures with lowest total energy values were taken as representative of solution conformations. None of these structures violated restraints by more than 0.2 Å.

Circular Dichroism

CD spectra were recorded on a JASCO J-715 spectropolarimeter. The instrument was calibrated with d(+)-10-camphor sulphonic acid. The path length used was 1 mm. The data were acquired in the wavelength scan mode, using a 1 nm band width with a step size of 0.2 nm. Typically, 8 scans were acquired from 260 to 195 nm using a scan speed of 50 nm/min. The resulting data were baseline corrected and smoothened. The peptide concentrations were 0.1 mg/mL.

X-Ray Crystallography

Single crystals of peptides **1** and **2** were grown from methanol/water and methanol/trifluoroethanol solutions, respectively. The crystal data for **1** are summarized in Table I. Peptide **2** [$P2_12_12_1$, a = 16.35(2) Å, b = 21.003(6) Å, c = 36.81(4) Å, Z = 8] did not scatter x-rays sufficiently well to derive a structure.

Table I Crystal and Diffraction Parameters of 1[a]

Empirical formula	$2(C_{46}H_{82}N_8O_{11}) \cdot H_2O$
Crystallizing solvent	CH_3OH/H_2O
Cocrystallized solvent	One H_2O/unit cell
Color/habit	Colorless thin laths
Crystal size (mm)	1.2 × 0.28 × 0.04
Space group	P1
a (Å)	9.942 (1)
b (Å)	11.240 (2)
c (Å)	25.882 (3)
α (deg)	86.14 (1)
β (deg)	95.62 (1)
γ (deg)	104.72 (11)
V (Å^3)	2780.5 (7)
Z	2
Mol. wt.	1862.1
Density (calc.; g/cm^3)	1.112
T (°C)	21
No. of unique reflections	9199
No. of obs. reflections., $\lvert F_o\rvert > 4\sigma F$	6997
R_1 (obs. data; %)	6.50
wR_2	0.1664
Resolution (Å)	0.9 Å
Data/parameter ratio	6.0
No. of parameters	1181
Residual elec. dens. (eÅ^{-3})	0.374 and −0.304

[a] CuK_α radiation (λ = 1.54178 Å) was used with a $\theta/2\theta$ scan, a scan width of 2.0° + $2\theta(\alpha_1 - \alpha_2)$, and a scan speed of 10 deg/min. Standard reflections were read every 97 measurements. Standards remained constant (within 3%).

Table II ^{1}**H NMR Parameters for Peptides** 1 **and** 2[a]

	δ (ppm)				Δ(δ) (ppm)[b]		$^3J_{NH—C^\alpha H}$ (Hz)	
	NH		$C^\alpha H$					
Residues	**1**	**2**	**1**	**2**	**1**	**2**	**1**	**2**
Leu(1)	6.68 (5.61)	6.72 (5.64)	4.21	4.20	0.32	0.24	9.0	8.8
Val(2)	7.93 (6.56)	7.93 (6.53)	4.80	4.78	0.45	0.68	9.3	9.3
Val(3)	8.88 (8.69)	8.77 (8.78)	4.50	4.60	−0.06	−0.10	9.2	8.6
D-Pro(4)	—	—	4.40	4.33	—	—	—	—
LAla/D-Ala(5)	8.68 (6.16)	7.37 (5.79)	4.35	4.33	0.50	0.38	8.0	6.1
Leu(6)	8.28 (7.83)	7.93 (7.21)	4.56	4.60	0.09	0.09	8.8	9.0
Val(7)	8.23 (6.52)	8.26 (6.47)	4.62	4.45	0.34	0.74	9.4	8.3
Val(8)	8.80 (8.39)	8.62 (8.39)	4.43	4.42	0.01	0.04	8.8	8.8

[a] Chemical shifts and coupling constants observed in CD_3OH solutions. The values in parentheses correspond to those in $CDCl_3$ solutions.
[b] $\Delta\delta = \delta(CDCl_3 + 10\%\ DMSO\text{-}d_6) - \delta(CDCl_3)$.

X-ray diffraction data were measured on a Siemens P4 automated four-circle diffractometer (presently called Bruker). Under a polarizing microscope, all the crystals for **1** exhibited twinning. The single crystal fragment used for data collection had to be cut out along a twin boundary from a larger crystal that appeared to have only one pair of twins.

The determination of the crystal structure of **1** was not entirely routine because it required 10,000 trials of direct phasing in the TREF routine found in the SHELXTL package of programs.[27] However, since the structure of peptide **3** was known,[14] in which the only difference between the sequence of **3** and **1** is an exchange of Gly^5 and L-Ala^5, respectively, an alternative procedure for determining the structure should be a rotation search in triclinic vector space (Patterson function) of a fragment of **3** that may resemble closely a portion of **1.** Accordingly, a 41 atom model comprising the backbone atoms and C^β atoms of one of the two independent molecules in the cell of **3** was chosen for the search. This process was not successful. After the structure of **1** was determined by the initial phase determining procedure above and shown that **3** and **1** are to a large extent isostructural and their cells are almost isomorphous, the rotation search was repeated. The same model was used but it was reduced to 26 atoms by eliminating atoms at the beginning and end of the sequence. This time the experimentally obtained rotational parameters, used in conjunction with the partial structure expansion procedure,[28] yielded the positions of 98 atoms out of a total of 131 atoms for the two independent molecules. The remaining atoms could be readily found in a difference map. The larger model used in the unsuccessful search procedure apparently had a sufficiently poor fit among the atoms near the ends of the two strands of the new β-hairpin so that the parameters obtained from the rotation search were corrupted. Experience has shown that fragments from known structures consisting of 20–30 atoms have the best rate of success in the vector search procedure.

Full-matrix least-squares refinements with anisotropic thermal parameters were performed on the coordinates of C, N, and O atoms. Hydrogen atoms were placed in idealized positions, and allowed to ride with the C or N atoms to which each is bonded. The side chains for Leu and Val residues had considerable

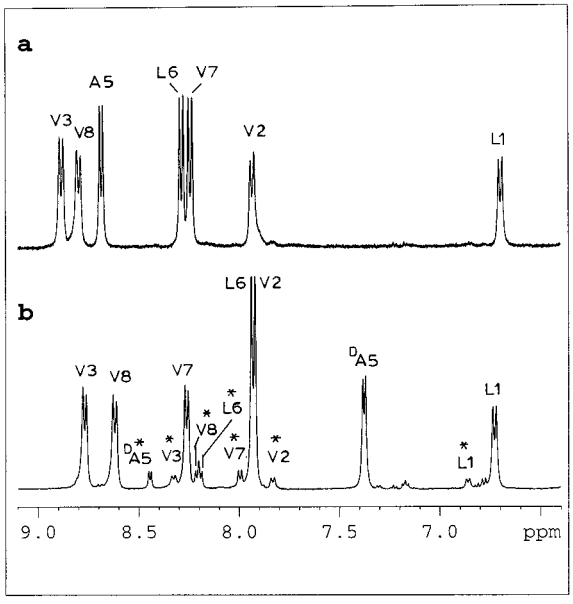

FIGURE 2 Partial 500 MHz ^{1}H NMR spectra for peptides **1** (a) and **2** (b) showing the amide (NH) resonances in CD_3OH (300 K). The starred resonances in (b) correspond to a population of minor conformer observed for peptide **2.**

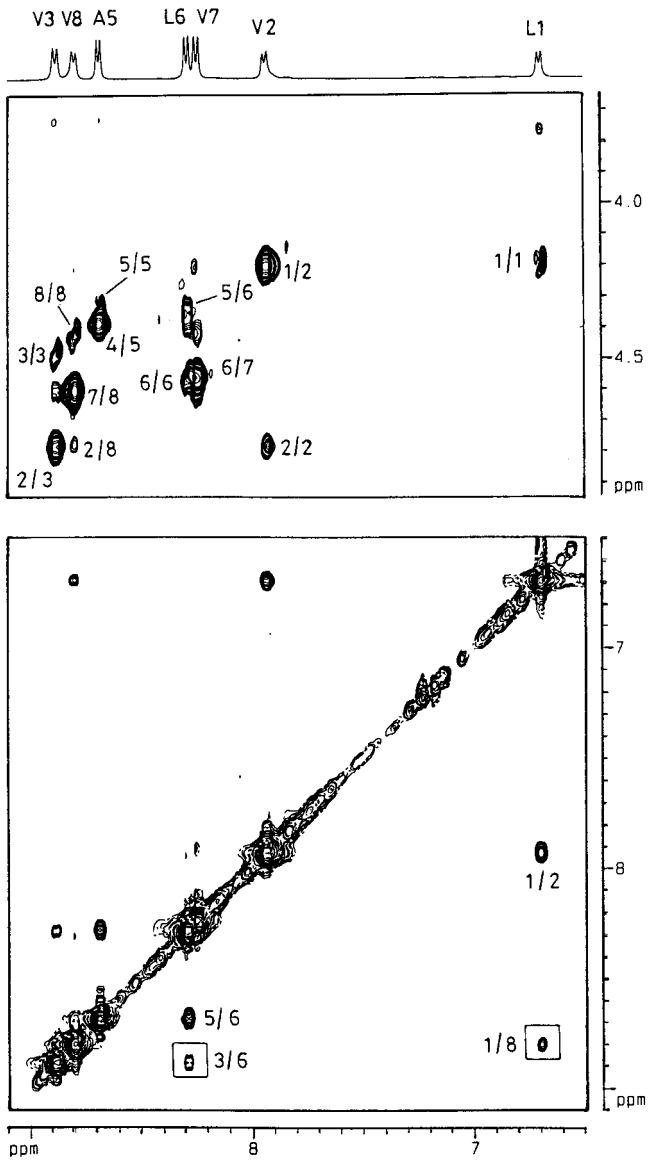

FIGURE 3 Partial 500 MHz ROESY spectra of peptide **1** in CD_3OH at 300 K. (Top panel) $C^{\alpha}H \leftrightarrow NH$ NOEs; (bottom panel) $NH \leftrightarrow NH$ NOEs. The residue numbers are used to label the cross peaks. Long-range NOEs diagnostic of β-hairpin conformations are boxed.

positional motion, especially near the C-terminals, as evidenced by large values for the thermal factors for atoms in the side chains. Initially, the least-squares refinements using F data with $|F| > 4\sigma$ were used, followed by refinements with F^2 data using all the observed data. There was no significant difference in the results. The results from F^2 refinements are reported. The conformation of the two independent molecules in the crystal of **1** are very similar. One of the molecules is shown in the stereodiagram in Figure 7. Fractional coordinates for **1** are deposited in the Cambridge Crystallographic Data Base.

RESULTS AND DISCUSSION

NMR Spectroscopy

Both peptides **1** and **2** were freely soluble in a variety of organic solvents and yielded well-resolved 500 MHz ^1H NMR spectra in chloroform-d_1 ($CDCl_3$), methanol-d_3(CD_3OH), and dimethylsulfoxide-d_6 (DMSO-d_6). In DMSO-d_6 a significant population of Val(3)–D-Pro(4) *cis* peptide conformations was observed, as previously noted for the D-Pro–Gly peptide.[15] Consequently detailed conformational analysis was restricted to methanolic solutions, while a limited

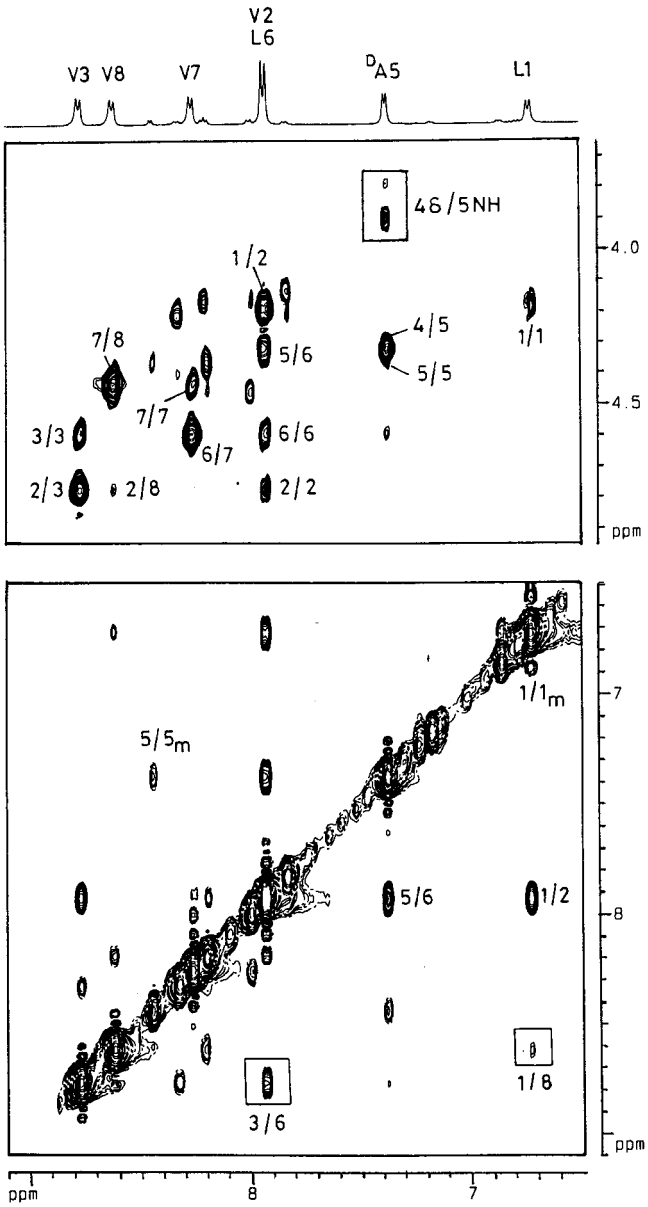

FIGURE 4 Partial 500 MHz ROESY spectra of peptide **2** in CD_3OH at 300 K. (Top panel) $C^{\alpha}H \leftrightarrow NH$ NOEs; (bottom panel) $NH \leftrightarrow NH$ NOEs. The residue numbers are used to label the cross peaks. Long-range NOEs diagnostic of β-hairpin conformations are boxed. The cross peak labeled $5/5_m$ corresponds to an exchange cross-peak between the D-Ala(5) NH resonances of the major and minor conformer.

comparison of NMR properties was made in chloroform. Sequence specific assignments were readily achieved by a combination of DQFCOSY and ROESY spectra.[29] Backbone proton chemical shifts (NH, and $C^{\alpha}H$) are summarized in Table II. Figure 2 shows a comparison of the distribution of NH resonances in the two peptides. In both cases the appearance of several NH resonances at extremely low field (<8.0 ppm) is indicative of hairpin conformations in which backbone protons on the extended strands are expected to be deshielded.[30] The $^3J_{NH—C^{\alpha}H}$ values listed in Table II for the six residues in the strand segments (1–3 and 6–8) are greater than 8.0 Hz, consistent with ϕ values characteristic of a β-sheet structure ($\phi \sim -120°$).[29,31] Comparison of NH chemical shifts reveals a striking difference for residue 5 (L/D-Ala) NH, which moves upfield by as much as 1.3 ppm on going from peptide **1** (L-Ala) to peptide **2** (D-Ala). A further point of interest is the observation of resonances corresponding to a minor conformation in peptide **2.**

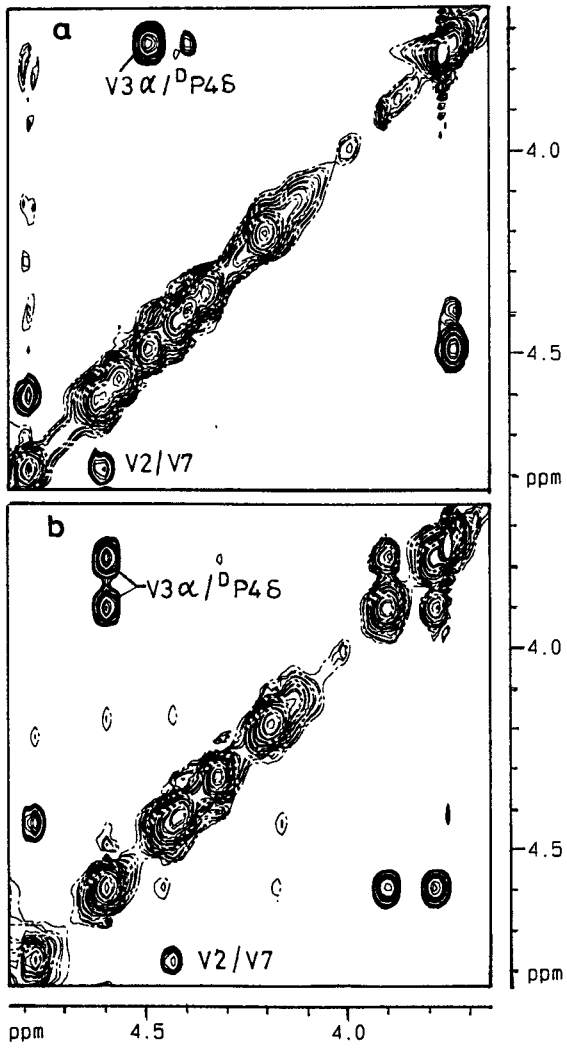

FIGURE 5 Partial ROESY spectra of peptides **1** (a) and **2** (b) illustrating $C^{\alpha}H$–$C^{\alpha}H$ and $C^{\alpha}H$–$C^{\delta}H$ NOEs observed for the peptides in CD_3OH (300 K).

The preponderance of β-hairpin structure in peptides **1** and **2** is conclusively established by the observation of all the relevant interstrand nuclear Overhauser effects (NOE). Figures 3 and 4 illustrate the backbone interresidue N_iH–$N_{i+1}H$ (d_{NN}) and $C_i^{\alpha}H$–$N_{i+1}H$ ($d_{\alpha N}$), and the intraresidue N_iH–$C_i^{\alpha}H$ ($d_{N\alpha}$) NOEs observed in **1** and **2.** The observed NOEs that support the deduced β-hairpin conformation are schematically indicated in Figure 1. It is readily seen that in both peptides $d_{\alpha N}$ interresidue NOEs are appreciably stronger than the corresponding intraresidue $d_{N\alpha}$ NOEs, consistent with extended (β) conformations at the residues 1–3 and 6–8. Furthermore, the interstrand Val(3) NH–Leu(6) NH and Leu(1) NH–Val(8) NH NOEs provide strong evidence for β-hairpin conformations. The only sequential NH–NH NOEs observed are the anticipated β-turn connectivity, Ala(5)–Leu(6), and the NOE at the N-terminus, Leu(1)–Val(2), which may be indicative of partial fraying of the structure. In the case of peptide **2,** exchange cross peaks of opposite phase are observed between the NH resonances of the major and minor conformations. Conclusive evidence for the β-hairpin conformation is obtained from the cross-strand $C^{\alpha}H$–$C^{\alpha}H$ NOE between Val(2) and Val(7) (Figure 5). The *trans* geometry of Val(3)–D-Pro(4) bond in both the peptides is also confirmed by the strong NOE between Val(3) $C^{\alpha}H$–D-Pro(4) $C^{\delta}H$ protons (Figure 5). The assignment of β-turn type in the two peptides rests critically on the NOEs observed at the D-Pro–Xxx segment. In the case of peptide **1** a strong $d_{\alpha N}$ NOE is observed between D-Pro(4) $C^{\alpha}H$–Ala(5) NH. This is consistent with a D-Pro ψ value of $\sim -120°$, which is compatible with the assignment of a type II′ β-turn conformation. In the case of peptide **2** a relatively intense NOE ($d_{\delta N}$) is observed between D-Pro(4) $C^{\delta}H$–D-Ala(5) NH protons. This NOE is consistent with a D-Pro ψ value of $\sim +30°$. It may be noted that the ϕ,ψ values of $+60°$, $+30°$ place D-Pro in a left-handed helical conformation, and the observed $d_{\delta N}$ NOE is formally analogous to the sequential d_{NN} NOE observed in the case of residues that bear an NH proton. Using idealized geometries the anticipated interproton distances calculated for the two turn types are as follows: $d_{\alpha N}$ (D-Pro–L-Ala) in type I′ = 3.55 Å, in type II′ = 2.20 Å; $d_{\delta N}$ (D-Pro–D-Ala) in type I′ = 2.74 Å, in type II′ = 5.50 Å. Using the experimentally determined NOE constraints, structures for both the peptides were computed which are illustrated in Figure 6 as an overlay of 10 structures with an RMSD of 0.37 Å for peptide **1,** and 0.36 Å for peptide **2**

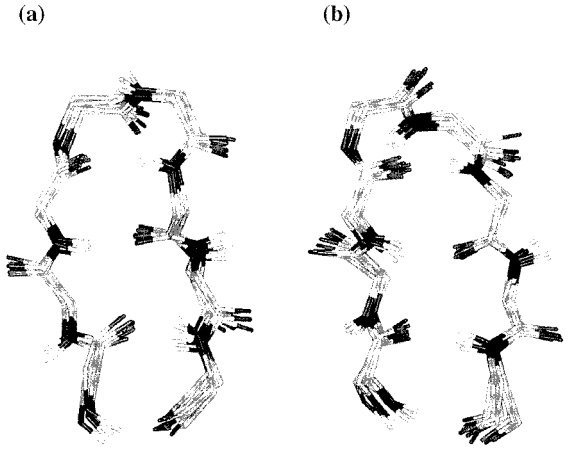

FIGURE 6 Superposition of 10 calculated structures based on NMR derived restraints for the peptides **1** (a) and **2** (b) showing the β-hairpin conformations in the peptides. The figure was generated using the program MOLMOL.[32]

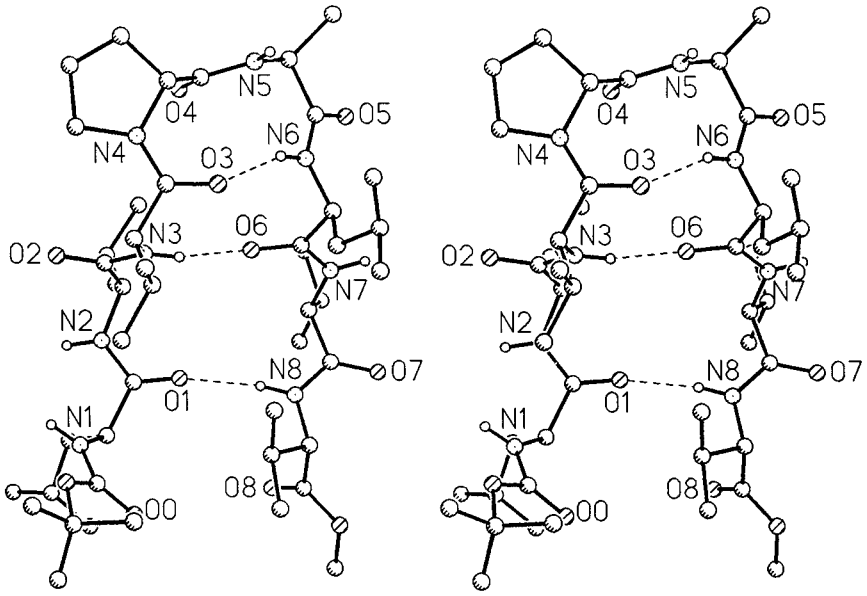

FIGURE 7 Stereodiagram of the molecular conformation in molecule A of peptide **1.** The independent molecule B in **1** is very similar.

(calculated for backbone heavy atoms using MOLMOL[32]). Peptide **1** (Xxx = L-Ala) adopts a β-hairpin nucleated by a type II′ β-turn, while for peptide **2** (Xxx = D-Ala) the NMR restraints are consistent with a hairpin initiated by type I′ β-turn.

The distribution of NH chemical shifts in $CDCl_3$ (Table II) suggests that β-hairpins are also predominantly populated, as anticipated, in the apolar solvent. In order to probe the involvement of the NH groups in intramolecular hydrogen bonding a limited solvent perturbation was carried out by addition of small amount of the hydrogen bonding solvent DMSO-d_6.[33] The solvent-induced shifts observed for NH protons on going from $CDCl_3$ to 10% DMSO-d_6 + $CDCl_3$ are listed in Table II. The Val(3), Leu(6), and Val(8) NH groups show negligible solvent dependence of chemical shifts as expected from their involvement in cross-strand hydrogen bonds (Figure 1). Of the remaining NH resonances Val(2) and Val(7) appear to be sensitive to solvent composition in both the peptides. Leu(1) shows a moderate solvent dependence, a feature consistent with the relatively exposed character of the terminal hydrogen bond in the hairpin. In both the peptides the L-Ala/D-Ala(5) NH at the β-turn is relatively exposed, showing significant solvent induced perturbation in the chemical shift.

The NMR results described above clearly support β-hairpin structures in both the peptides **1** and **2,** with the former incorporating a type II′ β-turn while the latter supports a type I′ β-turn. In accordance with analyses of hairpin structures in proteins the present study suggests that both "prime turn" types facilitate chain reversal with satisfactory interstrand registry. In the case of peptide **2,** a minor conformation ($\sim$ 10%) is observed in methanol solution. (Figure 2). Magnetization transfer by chemical exchange in ROESY experiments permits correlation of the backbone resonances of the major and minor conformations. While most NH resonances show small chemical shift differences between the major and the minor conformation, a large difference of 1.1 ppm is observed for D-Ala(5) NH, with a pronounced downfield shift of this resonance in the minor conformation. This observation suggests that the major and the minor conformations differ primarily at the stereochemistry of the turn segment. A tentative assignment of the minor conformer to a population of type II′ D-Pro(4)–D-Ala(5) β-turn is consistent with the observed chemical shifts. It should be noted that the type II′ structure will place D-Ala in the relatively less energetically favorable, right-handed helical, region of ϕ,ψ space. A similar distribution of major and minor conformers was also seen for peptide **2** in $CDCl_3$. Coalescence of resonances was observed upon heating to 323 K. In Pro-containing peptides detection of slowly exchanging conformation is often indicative of cis Xxx–Pro conformations.[34] This kind of conformational exchange is characterized by significantly higher barrier to interconversion ($\sim$ 20–22 kcal mol^{-1})[35,36] and is not compatible with the observed temperature of coalescence of resonances.

Crystal Structure

The two independent molecules A and B of **1** form an almost ideal β-hairpin structure with three interstrand hydrogen bonds, Figure 7. The fourth possible hydrogen bond within the hairpin between N1 and O8, does not occur because the N1H and N11H groups are rotated to the outside of the hairpins and form *inter* rather than *intra*molecular hydrogen bonds. Curiously, in the nearly isomorphous crystal[14] in which L-Ala(5) is replaced by Gly(5), one of the hairpin molecules has four intrastrand hydrogen bonds while the other is quite similar to the molecules in the present crystal. The conformations of the hairpin backbones in the crystal of **1** (Figure 7) are quite compatible with the conformation of **1** derived from solution data [Figure 6(a)]. Torsional angles and hydrogen bond parameters for molecules A and B are listed in Tables III and IV.

Each independent molecule in crystal **1** repeats along the crystallographic axis *a* and forms a separate extended beta sheet in which each strand is antiparallel to its neighbors (Figure 8). Hydrogen bonds N1 · · · O7a, N2 · · · O7a, and N7a · · · O2 for one molecule, and N11 · · · O17a, N12 · · · O17a, N17a · · · O12 for the other form between like molecules. At the β-turns the two independent strips of β-sheets are connected by means of the water molecule W with hydrogen bonds, that is N5aH · · · W1 · · · O14.

Circular Dichroism

The availability of short acyclic peptides adopting β-hairpin conformation provides an opportunity to investigate the circular dichroic properties of sequences which contain both short extended strands and a nucleating β-turn. Figure 9 shows the far uv CD spectra of **1** and **2.** The analogous octapeptide Boc–Leu–Val–Val–D-Pro–Gly–Leu–Val–Val–OMe (**3**) is also shown for comparison. Peptides **1** and **3** have been shown to adopt β-hairpin conformations nucleated by type II′ (D-Pro–Xxx) β-turns in the solid state (Ref. 14, and this study) and in solution (Refs. 13, 15, and this study). Both the peptides show a broad intense negative CD band at 215–218 nm with a crossover at ~ 197 nm. Interestingly, the spectrum of **1,** which contains an additional chiral center at the "*i* + 2" position of the β-turn, is more intense than that of peptide **3,** which contains the achiral Gly residue at this position. Peptide **2,** which has been shown in this study to favor a nucleating type I′ β-turn, has a dramatically different CD spectrum. The negative band at ~ 220 nm is much lower in intensity, with a crossover at appreciably longer wavelength (204 nm). A weak positive band at 196 nm is also detected. The

Table III Torsional Angles for the Hairpin Conformation of Boc–Leu–Val–Val–D-Pro-L-Ala–Leu–Val–Val–OMe in 1[a]

Residue	Angle	Molecule A, (degrees)	Molecule B,[b] (degrees)
		Backbone	
Boc(0)	ψ	+176	−179
	ω	+176	+179
Leu(1)	ϕ	−112	−110
	ψ	−57	−58
	ω	+176	+178
Val(2)	ϕ	−125	−111
	ψ	+111	+116
	ω	−169	−172
Val(3)	ϕ	−125	−130
	ψ	+105	+92
	ω	−172	−168
D-Pro(4)	ϕ	+62	+59
	ψ	−132	−135
	ω	+178	−180
Ala(5)	ϕ	−86	−80
	ψ	0	−8
	ω	−174	+177
Leu(6)	ϕ	−89	−77
	ψ	+139	+141
	ω	+167	+166
Val(7)	ϕ	−106	−122
	ψ	+110	+122
	ω	−175	−180
Val(8)	ϕ	−95	−76
	ψ	+147	+147
	ω	180	+176
		Side chains	
Leu(1)	χ_1	−69	+175
	χ_2	+173, −71	+65, −171
Val(2)	χ_1	−49, −171	+165, −71
Val(3)	χ_1	−58, +176	−174, −47
D-Pro(4)	χ_1	−10	−28
	χ_2	+3	+36
	χ_3	+5	−28
	χ_4	−12	+10
	$C4^{\delta}N4C4^{\alpha}C4^{\beta}$	+13	+11
Leu(6)	χ_1	−73	+164
	χ_2	+63, −176	+78, −172
Val(7)	χ_1	−55, +179	−58, +179
Val(8)	χ_1	−53, +177	−64, +170

[a] Torsional angles ϕ, ψ, and ω for the backbone and χ_n for the side chains follow the convention presented in Ref. 38. The estimated standard deviations are 1.0°–1.5°.

[b] Labels for atoms in molecule B differ from molecule A simply by the addition of the number 10.

NMR results reported in this paper clearly suggests that the nature of the β-hairpin conformation in peptides **1** and **2** are different, with a type II′ structure

Table IV Hydrogen Bonds in 1

Type	Donor	Acceptor	N · · · O and O · · · O (Å)	H[a] · · · O (Å)	Angle C═O · · · N (deg)
			Molecule A		
Inter	N1	O7[b]	2.955	2.10	154
Inter	N2	O7[b]	3.138	2.27	146
Intra	N3	O6	3.027	2.16	151
Peptide–water	N5	W1[c]	2.943	2.05	
Intra	N6	O3	2.965	2.11	135
Inter	N7	O2[c]	2.994	2.11	160
Intra	N8	O1	2.962	2.07	153
			Molecule B		
Inter	N11	O17[c]	2.920	2.06	151
Inter	N12	O17[c]	3.146	2.28	152
Intra	N13	O16	3.030	2.13	150
Inter	N15	O5[d]	2.882	1.98	127
Intra	N16	O13	3.037	2.25	133
Inter	N17	O12[b]	3.079	2.20	150
Intra	N18	O11	2.931	2.04	155
			Solvent		
	W1	O14	2.723		

[a] Hydrogen atoms were placed in idealized positions with N—H = 0.90 Å.
[b] At symmetry equivalent $-1 + x, y, z$.
[c] At symmetry equivalent $1 + x, y, z$.
[d] At symmetry equivalent $-1 + x, 1 + y, z$.

favored in the former while a type I′ turn is supported in the latter. The CD results in methanol suggest that the nature of the turn type may significantly affect the characteristics of the observed spectrum, which undoubtedly arises as a result of contributions from both the β-turn and antiparallel strands segments of the molecules.

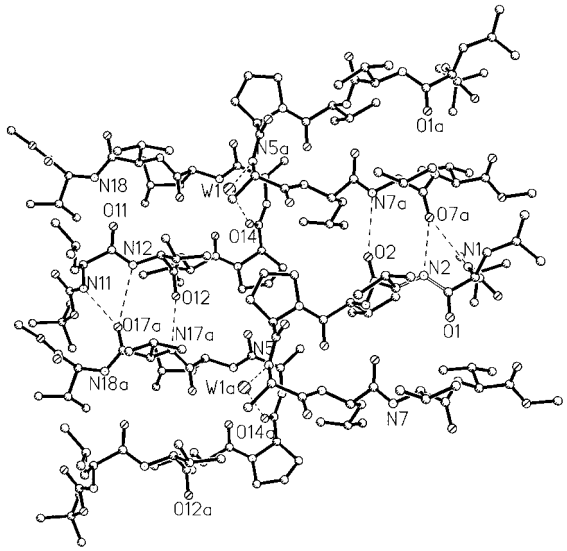

FIGURE 8 Packing view of **1** (down the *b*-axis), showing a continuous β-sheet formed by repeats along the *a*-axis. One set of independent molecules are shown on the right and the other set are shown on the left.

Figure 9 compares the CD spectra of **1–3** in 2,2,2-trifluoroethanol (TFE), a solvent in which measurements could be extended up to 182 nm. Clearly, the spectra of all three peptides resemble those obtained in methanol in the region 195–240 nm. The measurements in TFE permit clear observation of the low wavelength CD band that is centered at 187–190 nm in peptides **1** and **3,** and at 194 nm in peptide **2.** These CD spectra could provide a starting point for a theoretical analysis that attempts to dissect contributions from the distinct elements of backbone conformation that constitute β-hairpin conformations. Notably, vibrational CD (VCD) analysis of peptides **1–3,** which focused on the carbonyl stretching band at 1643–1655 cm^{-1}, revealed almost identical features in all these peptides.[37]

Conclusions

The results of the present study establish that peptide hairpins with appropriate cross-strand registry can be

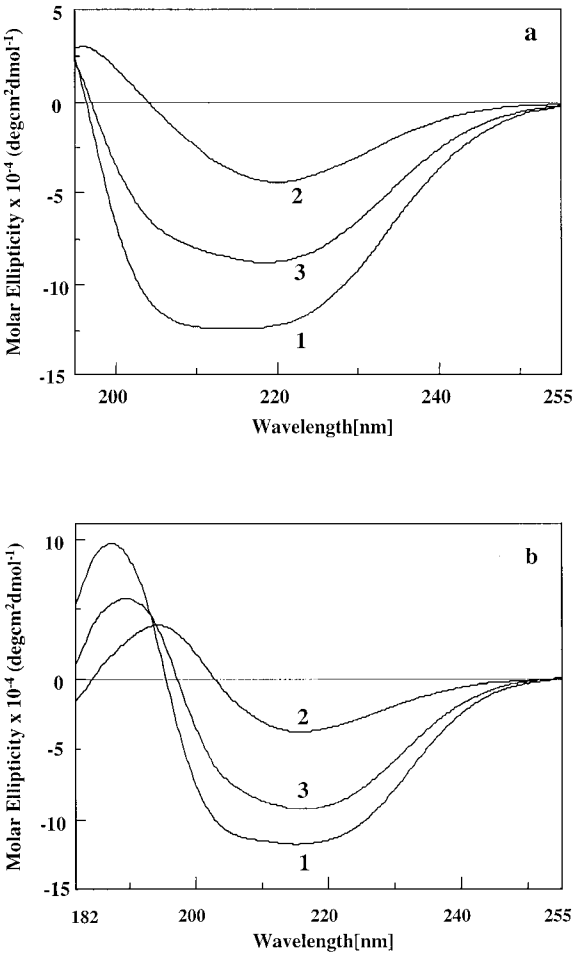

FIGURE 9 CD spectra of peptides **1** and **2** in the far uv region in methanol (a) and TFE (b) (300 K). Peptide **3** has the sequence Boc–Leu–Val–Val–D-Pro–Gly–Leu–Val–Val–OMe and was conformationally characterised in crystals and in solution (Refs. [13–15]). The β-hairpin conformation in this peptide is nucleated by a type II′ conformation at the D–Pro–Gly segment.

generated in sequences in which the sterochemistry at the tight turn is altered by a flip of the central peptide unit. The NMR studies demonstrate that the D-Pro–L-Ala segment nucleated a hairpin with a centrally located type II′ β-turn, while the D-Pro–D-Ala segment favors a type I′ β-turn. Limited evidence for a small population of type II′ β-turns in the case of D-Pro–D-Ala peptide has been obtained. These spectroscopic studies establish that interstrand hydrogen bonding is maintained irrespective of the nature of the turn type.

This research was partially supported by the program, Drug and Molecular Design, of the Department of Biotechnology, Government of India, and by National Institutes of Health Grant GM30902, USA, and the office of Naval Research.

REFERENCES

1. Sibanda, B. L.; Thornton, J. M. Nature 1985, 316, 170–174.
2. Sibanda, B. L.; Blundell, T. L.; Thornton, J. M. J Mol Biol 1989, 206, 759–777.
3. Gunasekaran, K.; Ramakrishnan, C.; Balaram, P. Protein Eng 1997, 10, 1131–1141.
4. Kaul, R.; Balaram, P. Bioorg Med Chem 1999, 7, 105–117.
5. Richardson, J. S. Adv Protein Chem 1981, 34, 167–330.
6. Srinivasan, N.; Anuradha, V. S.; Ramakrishnan, C.; Sowdhamini, R.; Balaram, P. Int J Pept Protein Res 1994, 44, 112–122.
7. Ramirez-Alvarado, M.; Blanco, F. J.; Serrano, L. Nature Struct Biol 1996, 3, 604–612.
8. Maynard, A. J.; Sharman, G. J.; Searle, M. S. J Am Chem Soc 1998, 120, 1996–2007.
9. Blanco, F. J.; Ramirez-Alvarado, M.; Serrano, L. Curr Opin Struct Biol 1998, 8, 107–111.
10. Haque, T. S.; Little, J. C.; Gellman, S. H. J Am Chem Soc 1994, 116, 4105–4106.
11. Haque, T. S.; Little, J. C.; Gellman, S. H. J Am Chem Soc 1996, 118, 6975–6985.
12. Haque, T. S.; Gellman, S. H. J Am Chem Soc 1997, 119, 2303–2304.
13. Awasthi, S. K.; Raghothama, S.; Balaram, P. Biochem Biophys Res Commun 1995, 216, 375–381.
14. Karle, I. L.; Awasthi, S. K.; Balaram, P. Proc Natl Acad Sci USA 1996, 93, 8189–8193.
15. Raghothama, S. R.; Awasthi, S. K.; Balaram, P. J Chem Soc Perkin Trans 2 1998, 137–143.
16. Struthers, M. D.; Cheng, R. P.; Imperiali, B. Science 1996, 271, 342–345.
17. Struthers, M. D.; Cheng, R. P.; Imperiali, B. J Am Chem Soc 1996, 118, 3073–3081.
18. Gellman, S. H. Curr Opin Chem Biol 1998, 2, 717–725.
19. Stanger, H. E.; Gellman, S. H. J Am Chem Soc 1998, 120, 4236–4237.
20. Chung, Y. J.; Christianson, L. A.; Stanger, H. E.; Powell, D. R.; Gellman, S. H. J Am Chem Soc 1998, 120, 10555–10556.
21. Seebach, D.; Abele, S.; Gademann, K.; Jaun, B. Angew Chem Int Ed Engl 1999, 38, 1595–1598.
22. Shankaramma, S. C.; Singh, S. K.; Sathyamurthy, A.; Balaram, P. J Am Chem Soc 1999, 121, 5360–5363.
23. Piantini, U.; Sorensen, O. W.; Ernst, R. R. J Am Chem Soc 1982, 104, 6800–6801.
24. Braunschweiler, L.; Ernst, R. R. J Magn Reson 1983, 53, 521–528.
25. Bax, A.; Davis, D. G. J Magn Reson 1985, 63, 207–213.
26. Bothner-By, A. A.; Stephens, R. L.; Lee, J.; Warren, C. D.; Jeanloz, R. W. J Am Chem Soc 1984, 106, 811–812.
27. Sheldrick, G. M. SHELXTL PLUS, Release 4.2 for Bruker R3m/V, Crystal Research System, Bruker Analytical X-Ray Instruments, Madison, WI, 1992.
28. Karle, J. Acta Crystallogr 1968, B24, 182–186.

29. Wüthrich, K. NMR of Proteins and Nucleic Acids; Wiley: New York, 1986.
30. Wishart, D. S.; Sykes, B. L.; Richards, F. M. J Mol Biol 1992, 222, 311–333.
31. Pardi, A.; Billeter, M.; Wüthrich, K. J Mol Biol 1984, 180, 741–751.
32. Koradi, R.; Billeter, M.; Wüthrich, K. J Mol Graphics 1996, 14, 51–55.
33. Iqbal, M.; Balaram, P. J Am Chem Soc 1981, 103, 5548–5552.
34. Grathwohl, C.; Wüthrich, K. Biopolymers 1976, 15, 2025–2041.
35. Fischer, S.; Dunbrack, R. L. Jr.; Karplus, M. J. Am Chem Soc 1994, 116, 1193–11937.
36. Rabenstein, D. L.; Shi, T.; Spain, S. J Am Chem Soc 2000, 122, 2401–2402.
37. Zhao, C.; Polavarapu, P. L.; Das, C.; Balaram, P. J Am Chem Soc, submitted.
38. IUPAC-IUB Commission on Biochemical Nomenclature. Biochemistry 1970, 9, 3471–3479.